

Differential tunneling spectroscopy simulations: Imaging surface states

W. A. Hofer* and A. Garcia-Lekue

Surface Science Research Centre, Department of Physics, University of Liverpool, Liverpool L69 3BX, United Kingdom

(Received 19 August 2004; revised manuscript received 19 October 2004; published 1 February 2005)

We present a method to simulate scanning tunneling spectra on metal and semiconductor surfaces. The method is based on the full electronic structure of the surface and the tip. Compared to existing methods, it provides the additional advantage that surface and tip contributions can be clearly distinguished in the ensuing spectrum. Analyzing the spectra of surface states on (111) noble metal surfaces, we find that the simulations agree well with experimental data only with respect to the surface contributions. We conclude that model tips in spectroscopy simulations have to be modified compared to the tips used in topography simulations in the past.

DOI: 10.1103/PhysRevB.71.085401

PACS number(s): 73.23.Hk, 72.10.Bg, 72.15.Eb

I. INTRODUCTION

Experiments in scanning tunneling microscopy (STM) over the past ten years have increasingly moved from an analysis of structure and atomic positions to an analysis of electronic properties and processes. The main reason for this change of focus is the wide availability of low-temperature (about 80–200 K) and even very-low-temperature (mK to a few K) microscopes. The new level of experimental precision has had some remarkable consequences in research. In particular, the demonstration of standing-wave patterns of surface electrons, e.g., on Ag(111),^{1–3} images still used for the cover design on nanotechnology books, has come to symbolize, more than other measurements, the instrument's power and precision. In a wider frame of reference, tunneling spectroscopy, due to its rich features and resolution power of complex electronic properties, is probably the most expansive field in low-temperature STM experiments today. This evolution clearly indicates that the field has sufficiently matured. High-resolution topographies and numerical simulations are now all but routine, and, apart from the so far unsolved problem of assessing the agreement between experimental and simulated STM tip models, the correspondence between experiment and theory is satisfactory if not, in some cases, spectacular.^{4,5}

To move theoretically in the same direction as low-temperature experiments, i.e., to go from topography to high-resolution spectroscopy, poses some particular problems, once theory tries to progress beyond the description of the surface alone. The surface alone and its characteristics in tunneling spectra can be inferred from the local density of states and its changes with bias voltage. But if a simulation is to include the whole tunneling junction and not just one part of it, it is immediately confronted with the problem of tip representation. It is quite well known that metal surfaces frequently possess a rather complicated band structure near the Fermi level.⁶ In an experimental spectrum, the features will be determined not only by the surface itself, but also by the STM tip. Experimentally, a way around this problem is the preparation of specific blunt tips,⁷ which can be gauged on particular systems, e.g., Cu(111), where the signature of the surface electronic structure is well known. Theoretically, a similar strategy needs to be adopted if one does not know,

initially, the detailed structure of the STM tip used in spectroscopy experiments. In spectroscopy, the parameter space for tip simulations is substantially larger than in topographies, because one crucial property of tips in high-resolution topographic experiments is missing. Spectroscopy tips do not usually yield atomic resolution of a flat metal surface, which suggests that they *cannot* possess a mono-atomic apex. This removes many of the constraints used to great profit in topography simulations. As the current is no longer passing through a single apex, the theoretical problem can no longer be reduced to finding a particular chemical composition, e.g., a contamination on a tungsten base,⁸ but is also confronted with the exact geometry and termination of a large array of atoms. The parameter space in this case increases beyond what is numerically manageable. That is to say, even though one can in principle construct tip models of a few hundred atoms with today's computer codes, it is unfeasible to map the ensuing band structure with suitable resolution.

How does the resolution of a spectrum relate to the map of the band structure? Assuming that the energy resolution in today's best experiments is in the range of mV,³ a numerical representation of the experiment has to include, for a specific band, at least one k point of the surface Brillouin zone every few mV. This makes, e.g., on a noble metal surface, for a few thousand k points of the band-structure map. On a known surface, one could circumvent the problem by some clever interpolation routine. However, on an unknown or electronically very complicated, e.g., magnetic, surface, this might not work too well and shift the problem mainly to a different arena, without actually reducing the numerical effort. Given this level of precision, the parameter space for accurate tip calculations becomes so large, and the calculations so expensive, that they would actually be unfeasible for routine simulations of spectroscopy experiments.

For these reasons, we have adopted a two-way strategy. On the one hand, we have developed numerical spectroscopy simulations based on the Bardeen method, shown to be very reliable in topography simulations.^{4,9} On the other hand, we have also developed a direct way to determine the changes from one bias value to the next. This method allows us to separate the effects of surface and tip electronic structure. The main conclusions of our simulations of noble metal surfaces are as follows: (i) Simulated spectra are at present pre-

cise enough for detailed comparisons with state-of-the-art experiments in the temperature range above 150 K; and (ii) the electronic structure of the tip models tested is unsuitable to represent the tips in the experiments. The paper is organized as follows. In Sec. II, we shall briefly talk about the computational methods and the main equations of Bardeen and differential spectra. Section III shows our simulated results for the spectra on noble metal (111) surfaces. The final sections present a discussion of results and a summary of the work.

II. THEORY AND NUMERICS

A. Differential tunneling spectroscopy simulations

The central theoretical formulations of Bardeen's approach to tunneling are well known. Their main equation describes the dependency of the tunneling current on the bias voltage V and the position of the STM tip \mathbf{R} . It is usually written^{4,9}

$$I(\mathbf{R}, V) = \frac{4\pi e}{\hbar} \sum_{ik} \int_0^{eV} dE [f(\mu_S, E - eV) - f(\mu_T, E)] \times \left| -\frac{\hbar^2}{2m} M_{ik} \right|^2 \delta(E_i - E_k). \quad (1)$$

Here, $\mu_{S(T)}$ denotes the Fermi function of the surface (tip). The δ functional in this equation is due to energy conservation, which is a central assumption in the derivation of the formula, e.g., from the separate wave functions of surface and tip in Chen's modified Bardeen approach.¹⁰ In principle, the relation can be used for any bias voltage within a range of about ± 1 V, where the change of electronic properties of the sample surface due to the potential of the tip is sufficiently small and well below the range of field emission. The set point of a given spectroscopy measurement is determined by the current at a specific bias voltage. Usually, the current feedback loop is then disengaged and the bias voltage changes over a specific range. It is thus only by performing the integration that one actually knows the distance of the STM tip from first principles.

Here, we encounter two fundamental theoretical problems. First, experimental results are usually given in terms of dI/dV curves, which will involve the numerical differentiation of Eq. (1). The differential value cannot directly be obtained, e.g., from the integral kernel, without some approximations involved, since a change of bias will also change the transition channels by virtue of the δ functional. Such a numerical differentiation, however, will make the calculation inherently unstable due to the Fermi distribution functions. As the largest slope of the current will be found near the Fermi level, this region will always prominently show up in the computed spectrum. An obvious solution to the problem is to compute the spectra for zero temperature. In this case, the Fermi distribution functions are changed to step functions and electrons of both systems will always tunnel strictly from an occupied into an unoccupied state.

The second problem is a problem of control: the numerical differentiation procedure does not allow any distinction

between states of the surface and states of the tip. The ensuing $I(V)$ distribution and its numerical derivative are therefore convolutions of surface and tip states. The electronic structure of both sides of the tunneling junction contributes in an equal manner to the result. A solution to this problem would be to revert back to the Tersoff-Hamann model of tunneling.¹¹ There, the current is assumed proportional to the local density of states of the surface by virtue of an approximation for the tip states, viz., the only involved tip state is a state of radial symmetry, and such a tip state exists for every bias voltage. The voltage dependency can be included by a model suggested by Lang,¹²

$$\frac{dI}{dV} \propto e\rho_S(\epsilon_F + eV)T(\epsilon_F + eV, V) + \int_{\epsilon_F}^{\epsilon_F + eV} \frac{d}{dV} [\rho_S(\epsilon)T(\epsilon, V)] d\epsilon. \quad (2)$$

ρ_S denotes the local density of surface states at the vacuum boundary z_s , and $T(\epsilon, V)$ is the transmission coefficient through an average barrier at a given bias voltage and energy ϵ ; it is described by

$$T(\epsilon, V) = \exp\left[-2s\sqrt{2m(\Phi_{av} + \epsilon_F - \epsilon + eV/2)/\hbar}\right]. \quad (3)$$

The average work function $\Phi_{av} = (\Phi_S + \Phi_T)/2$, while s is the vertical distance between the tip apex and the vacuum boundary z_s of the surface. In the limit of zero bias, only the first term survives, and the expression reduces to the usual formulation within the Tersoff-Hamann approximation,

$$I(\mathbf{R}, V) \propto \int_0^{eV} dE \sum_i |\psi_i|^2. \quad (4)$$

In this case, the integral kernel and thus the dI/dV spectrum can be directly determined since the eigenvalues or the transition channels are only related to the bias interval and are incrementally increased for an incremental increase of the bias voltage. However, it should be clear that the spectrum obtained from the integral kernel is qualitatively different from the spectrum, e.g., obtained by the Bardeen method and a numerical differentiation. While the first could be called a differential spectrum, the second is the derivative of an integral spectrum. For reasons of consistency, the assumption that current is proportional to the local density of states, which is at the bottom of the Tersoff-Hamann model, finds its expression here in the proportionality of the current derivative and the derivative of the local density of states.

This might seem an unnecessarily fine distinction, but it is also made in experimental spectra. Early experiments, e.g., by Stroscio and Biedermann,^{13,14} determined the dI/dV curve by numerically differentiating a measured $I(V)$ curve. Numerical differentiation of noisy data is generally problematic. It is thus that the method works comparatively well in an ambient environment and for very distinct electronic features of a surface, e.g., a surface state on Fe(001) or Cu(111). It fares far worse in the determination of subtle features, e.g., the onset of a surface state in low-temperature experiments or the threshold of a vibrational node in single-molecular spectroscopy. There, the incremental differences are directly

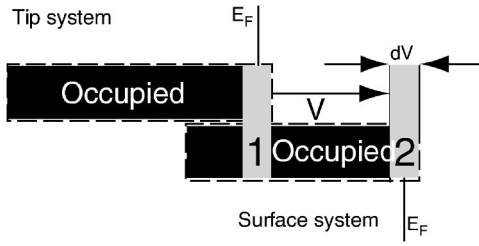


FIG. 1. Contributions to the tunneling current at a bias voltage V . The change of the bias by an incremental value dV leads to two distinct additional contributions (gray): one contribution mapping the states at the Fermi level of the tip onto the band structure of the surface (1), and one contribution mapping states at the Fermi level of the surface onto the band structure of the tip (2).

determined by oscillating the bias voltage around a median value by about 20 mV.¹⁵ Since the actual changes here occur in a range of only 20 mV, it becomes unfeasible to account for experimental results by integral spectroscopy.

A short example might illustrate the issue. It is well known that the surface state of Cu(111) is located at about -450 mV from the Fermi level at the Γ point of the surface Brillouin zone. It is equally well known that the dispersion of the state leads to a k vector of about $0.5\pi/a$ at the Fermi level. If the spectrum from -450 to 0 mV should possess a resolution better than 10 mV, then the interval must be spanned by at least 100 k points, due to the requirement of numerical stability in the differentiation. This, in turn, means that the Brillouin zone has to be mapped by more than 100 000 k points. Not only is it close to impossible to perform such a calculation within density-functional theory, given standard size computer systems, it also seems highly inefficient. The ensuing spectrum, precise though it might be, still does not answer the question of what actually causes a particular feature in the spectrum. The origin still could be both the copper surface or the STM tip.

To account for both problems—the problem of high resolution and the problem of identifying a particular feature—we need to develop a method, similar to a determination of the spectrum from the integral kernel alone, but for a calculation including the STM tip. The solution could be called a differential Bardeen spectrum, and it rests on one approximation: a change of the bias by an incremental amount leaves the bulk of the transition channels unchanged. The only changes are the additional transitions due to the change of bias voltage. The incremental current change in this case has two distinct components: one component due to overlaps of states at the Fermi level of the tip and states of the band structure of the surface, and one component mapping states at the Fermi level of the surface to the band structure of the tip (see Fig. 1). The method deviates to some extent from the method suggested by Hörmandinger a few years ago. There, the derivative of the current with respect to voltage was described by¹⁶

$$\frac{dI}{dV} = f_T(0)f_S(eV) - \int_0^{eV} dE f_T'(E - eV)f_S(E). \quad (5)$$

The functions $f_S(T)$ of the surface (tip) electronic structure denote the contributions to the tunneling matrix element in the Bardeen approach, and it was assumed that these contributions can be split into products. In this paper, we follow a different approach for two reasons. (i) The expression still contains a derivative with respect to the bias of the tip contributions. It will be seen in our analysis of simulated results that such a derivative is inherently numerically unstable and requires a map of the tip band structure beyond today's computational means. (ii) The integral kernel in the Bardeen matrix element contains the expression $(\chi^* \nabla \psi - \psi \nabla \chi^*)$. It seems not feasible to separate the ensuing square of the surface integral in separate surface and tip functions, or only if one assumes a featureless tip which can be described analytically.

Apart from making the separate contributions identifiable, the suggested method for differential spectroscopy has two additional advantages: since it does not involve a numerical differentiation it is also more stable and more precise; and since it involves at each step only a fraction of the actual bias voltage range, it is also considerably faster. The numerical values in such a calculation, however, are still actual values, e.g., in nA/V, and can therefore directly be compared to experimental results. The incremental change in the current due to a change of bias from V to $V+dV$ is then

$$dI = \sum_{i_1 k_1} |M(\psi_{i_1}, \chi_{k_1})| + \sum_{i_2 k_2} |M(\psi_{i_2}, \chi_{k_2})|, \quad (6)$$

where the eigenvalues of surface $E_{i_{1(2)}}$ and tip $E_{k_{1(2)}}$ states are within the intervals

$$E_{i_1} \in [E_F + eV - edV/2, E_F + eV + edV/2],$$

$$E_{k_1} \in [E_F - edV/2, E_F + edV/2],$$

$$E_{i_2} \in [E_F - edV/2, E_F + edV/2],$$

$$E_{k_2} \in [E_F - eV - edV/2, E_F - eV + edV/2]. \quad (7)$$

Here, E_F denotes the Fermi level of the surface and tip system, respectively. Then the total spectrum contains equally two distinct contributions due to the band structure of the surface and the tip system,

$$\frac{dI(V)}{dV} = \sum_{i_1 k_1} \frac{|M(\psi_{i_1}, \chi_{k_1})|}{dV} + \sum_{i_2 k_2} \frac{|M(\psi_{i_2}, \chi_{k_2})|}{dV}. \quad (8)$$

In this case, the simulated values are very stable, since a constant bias increment has the effect that the surface band structure always maps onto the same STM tip states at the Fermi level. Any changes from one bias value to the next are therefore directly related to the changes of the surface electronic structure. Numerically, the calculation is also very efficient: given a high resolution of the surface and tip Brillouin zone and a small bias increment of about 5–10 mV, the simulation of one point of a spectrum can be performed, on a workstation, within less than 1 h. This, in turn, makes it possible to simulate tunneling spectra also with high local resolution.

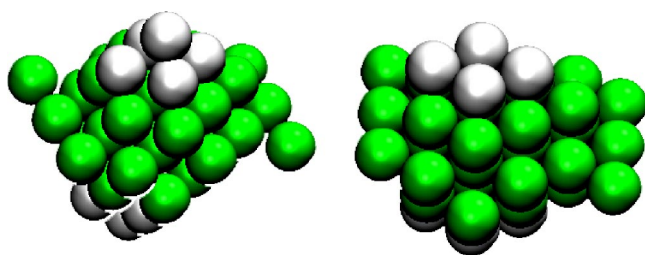


FIG. 2. (Color online) The two STM tip models used in the simulations. The models are based on a three-layer tungsten film in (110) orientation (dark atoms), covered by a tungsten pyramid (left, bright atoms) or a tungsten tetramer (right).

B. Calculating the surface electronic structures

The electronic structure of noble metal surfaces and model tips was calculated with density-functional methods. We used the Vienna Ab Initio Simulation Program (VASP).^{17,18} The potentials of the ionic cores were modeled with VASP's projector augmented-waves (PAW) (Ref. 19) implementation. The exchange correlation energy was calculated within the PW91 parametrization scheme.²⁰ Initially, we calculated the electronic structure of 13-layer films, separated by 15 Å of vacuum. We found that in this case the surface states of the film couple through the bulk as well as the vacuum, leading to two surface states on either side with an energy difference of 10 mV. The number of layers was therefore increased to 25 [Ag(111)], or one surface of the film was passivated by hydrogen adsorbed in the threefold hollow sites [for Cu(111) and Au(111)]. This measure was suitable to either reduce the splitting of the surface bands to less than 1 meV [Ag(111)], or to quench the surface electrons on one surface. Similar results were previously found by full-potential calculations of the Au(111) and Ag(111) surface states.²¹ It should be mentioned that we used the experimental lattice constant in all calculations, as previous experience with a theoretical lattice constant indicates that, e.g., the surface state of Ag(111) is shifted into the unoccupied range. All surfaces were fully relaxed. The electronic ground state and the charge distribution were calculated with a Monkhorst-Pack grid of $10 \times 10 \times 1$ special k points in the irreducible wedge of the surface Brillouin zone. In the final calculation, we used a k map centered at the Γ point of 331 special points within the irreducible wedge covering only 25% of the full Brillouin zone. This is sufficient to map the surface bands on all surfaces up to about 1 eV above the Fermi level. The final map amounts to more than 2000 points at the center and a correspondingly high resolution of the metal band structure.

The STM tip models in the simulations were tungsten (110) films terminated either by four tungsten atoms (flat tip) or by four tungsten atoms and a single atom at the apex (sharp tip). Also in this case, the systems were fully relaxed. Since the tip unit cells are significantly larger than the surface unit cells, we only used 100 k points centered at the Γ point to map the tip electronic structure. The atomic arrangement of the two tip models is shown in Fig. 2.

C. Calculating the tunneling spectra

The calculation of tunneling spectra with the method described above is straightforward. The bias voltage is ramped

from an initial value (-1 V) to a final value ($+1$ V) in steps of 20 mV. At every step the incremental change is calculated. We only present results for one STM tip position on the surface: the position on top of surface atoms. The results for the hollow positions differ only slightly by their absolute values (less than 1% in the distance range of evaluation). The set point for the evaluation, which corresponds to the point in the experiments, where the feedback loop is disengaged, was set to a distance of 7.0 Å between the surface and the STM tip. In this range, currents are sufficiently small (less than 1 nA at a bias of -1 V) so that interactions between surface and tip can be safely neglected. The dI/dV spectra were finally smoothed with Gaussian of 20 mV, 50 mV, and 80 mV half-width, respectively.

III. DIFFERENTIAL SPECTRA ON NOBLE METAL SURFACES

The (111) surfaces, of copper, silver, and gold have been researched extensively due to their importance as model systems for two-dimensional electronic structures. The silver (111) surface, where the bottom of the surface state band lies very close to the Fermi level, also allows us to study interference of surface electrons scattered at atomic centers or step edges. The reason, in this case, is the long wavelength of surface electrons at the Fermi level, which is substantially larger than the dimension of the unit cell. In this case, the interference pattern dominates STM images, and the decay, e.g., from a step edge, can be used to estimate the lifetime of surface-state electrons due to their interactions with electrons and phonons of the crystal. The copper (111) surface is one of the main systems in surface-science research for three reasons: it is easy to clean and then provides large flat terraces which can be measured by scanning probe or electron diffraction methods; it does not interact easily with adsorbates and can therefore be used to study the processes occurring during alloying with other metals; and it is one of the easiest systems to measure with STM due to the relatively high corrugation of 10–20 pm. Apart from that, its surface state is easily recognized even under ambient conditions. The gold surface is important in two separate fields. In nanoelectronics, it is used as the conducting material, e.g., in circuits comprising organic molecules or single organic films positioned between gold electrodes. Such a setup has potentially important applications in organic transistors. In heterogeneous catalysis, it was found recently that small clusters of gold on, e.g., titanium oxide templates provide a much enhanced catalytic performance.²² There seems to be still some controversy, whether this enhancement is due to catalytic processes at the rims of the cluster, or whether the strain on the gold films changes their electronic properties in such a way that the interaction with physisorbed molecules changes significantly.²³ Copper and gold surface states have been most successfully mapped by angle-resolved photoemission experiments,²⁴ while low-temperature STM measurements have been used to determine the onset and thus the lifetime broadening.³ In all three cases, detailed spectroscopic simulations have so far not been performed; the best theoretical data result from one-dimensional models including many-body effects.²⁵

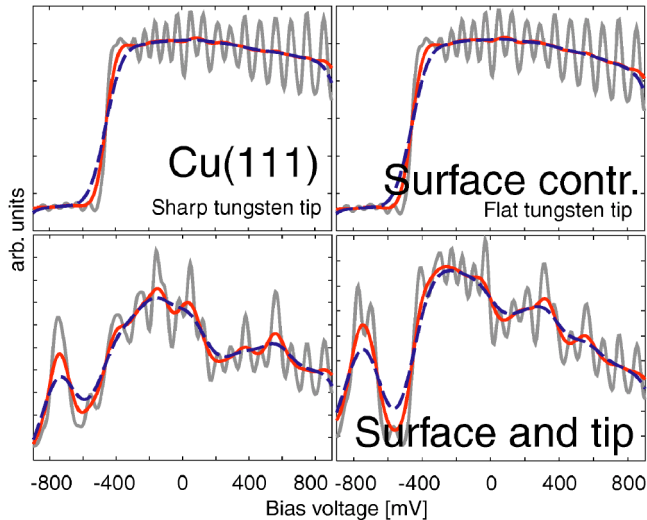


FIG. 3. (Color online) Differential spectrum on Cu(111). The top frames show the surface contribution of the spectrum, simulated with the sharp (left) and flat (right) tip. The bottom frames display the sum of surface and tip contributions. Results are given for three different values of thermal broadening: 20 mV (gray), 50 mV (solid line), and 80 mV (dashed line). It can be clearly seen that the tip contribution for the chosen model tips leads to a peak at about -800 mV, in contrast to experiments.

A. Tunneling spectra on Cu(111)

The differential spectra on Cu(111) are shown in Fig. 3. The top frames represent the surface contributions only. The left frames are the simulated spectra with an atomically sharp tungsten tip; the right frames show the spectra for a flat tip. We simulated the ensuing spectra under different thermal conditions, included in the evaluation by a broadening of spectral features with a Gaussian of 20 mV (gray), 50 mV (full line), and 80 mV (dashed line) half-width. Initially we note that the top frames for the two spectra are identical. The only difference is the absolute values, which depend on the number of states at the Fermi level of the STM tip. It can be seen that this has no influence on the onset of the surface state at about -450 mV. The oscillations of the spectrum with a period of about 25 mV denote the energy resolution in the simulation. Decreasing the broadening to less than 20 mV thus will not affect the ensuing spectrum. Considering the overall shape of the spectrum, it can be seen that it is rather similar to a step function. If the thermal broadening is increased to about 50 mV, the oscillations due to the discrete k mesh in the simulation vanish. It may thus be concluded that the spectrum yields an accurate description of experiments at temperatures above 150 K.

The bottom frames show the spectra including the band structure of the STM tip. We notice two features which are due to the tip electronic structure alone: (i) a peak at about -800 mV and (ii) a dip at the Fermi level. Both of these features are not confirmed by experimental data.²⁶ They clearly indicate the limitations of the tip models used in the simulations. Given that the peaks in the full spectra are unequally spaced, the additional features should not be due to

the limited k grid of the tip used in the simulations. The effective area of the k mesh was limited to about 25% of the tip Brillouin zone. If this were the origin of the additional peaks, then under the condition of equally spaced d bands the peak would reveal an equal distribution with respect to energy. However, the difference between the first peak at -800 mV and the second or third not only varies in value, it also varies from one tip to the other. We conclude from this feature that the additional peaks, distorting the spectrum of the surface electronic structure, are due to the limitation of our tip unit cell and the confinement of electrons to comparatively few film layers. The same conclusion could be drawn by a comparison with the spectra on Ag(111) or Au(111), which reveal the same additional peaks, also varying from the sharp to the flat STM tip model. There is, however, one feature of the spectrum including the STM tip, which has a profound physical meaning. It can be seen, in particular by comparing the full spectrum for the combined flat tip and surface with the spectrum of the surface alone, that the former shows a slope toward higher energy values which does not exist in the latter. This effect is genuine: when the surface states map onto tip states with lower energy, as the energy is increased, the decay length of the tip states becomes shorter and thus the overlap with surface states smaller. The dispersion of the surface state, which leads to a change of the electron momentum in the z direction, and the height of the vacuum barrier at a specific energy uniquely characterize the decay length of surface-state electrons. As it remains fairly constant over the bias range, as revealed by the spectrum of the surface state alone, the additional tip contribution leads to a slope toward higher bias values, which is also confirmed by experiments.²⁶

B. Tunneling spectra on Ag(111)

On Ag(111), the simulations including only the surface electronic structure and the states at the Fermi level of the STM tip show an onset of the surface state around -80 mV to -70 mV, indicating the bottom of the surface band. In this case, the spectrum also shows a slope toward higher bias values. We conclude from this difference that the one-dimensional picture, which unambiguously assigns a step-function behavior to the spectrum of surface states, needs to be modified in a three-dimensional environment. As the decay of the surface-state electrons into the vacuum depends on an interplay between the dispersion of the state and the decay characteristics due to the vacuum barrier, it is subject to differences for different metals. In a simplified model, we may write for the relation between the vacuum decay constant κ , the energy eigenvalue E , and the reciprocal-lattice vector k (in atomic units),

$$\kappa^2 - k^2 = 2E, \quad E = E_0 + \alpha k^2, \quad (9)$$

where α is characteristic for the dispersion of a particular surface state. If we assume that the differential contribution to the tunneling current at a specific bias voltage and distance z_0 depends on the vacuum decay length κ and the area of the Brillouin zone covered in a particular energy interval, the differential change of the current will be

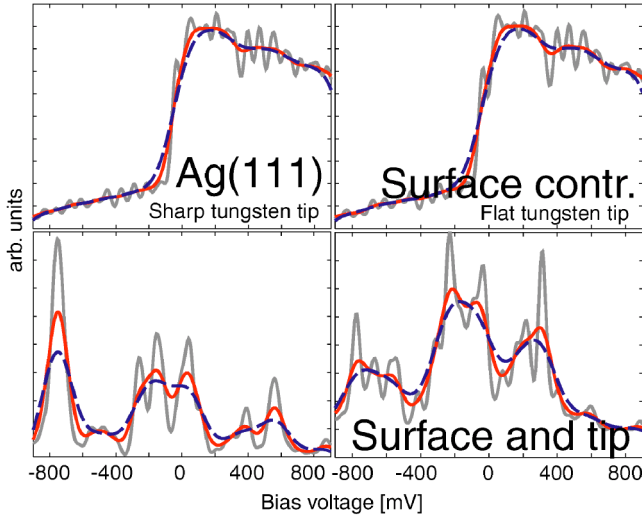


FIG. 4. (Color online) Differential spectrum on Ag(111). The top frames show the surface contribution of the spectrum, simulated with the sharp (left) and flat (right) tip. The bottom frames display the sum of surface and tip contributions. It can be clearly seen that the tip contribution in this case distorts the spectra and makes the onset of the surface state all but unrecognizable.

$$dI(k) = \exp\left(-z_0 \sqrt{E \frac{1+2\alpha}{\alpha} - \frac{2E_0}{\alpha}}\right) 2k\pi dk. \quad (10)$$

The relation between bias voltage and energy is given by

$$E = E_F + V. \quad (11)$$

Then conductance, or dI/dV , will be described by

$$\frac{dI}{dV}(z_0, V) = \frac{\pi}{\alpha} \exp\left(-z_0 \sqrt{V \frac{1+2\alpha}{\alpha} + \text{const}}\right). \quad (12)$$

The spectrum will show a slope as the bias voltage is increased. The slope depends on the energy of the surface state at the center of the Brillouin zone E_0 , and the surface state dispersion α , and will differ for different surface states.

The results of our simulation on Ag(111) are shown in Fig. 4. The slope is considerably larger in the positive bias regime than, e.g., for Cu(111). Also in this case the surface contributions alone are in good agreement with experiments, while including the tip band structure in the differential spectrum leads to artificial peaks at -800 , -200 , and $+500$ mV (sharp tip), or -800 , -200 , and $+300$ mV (flat tip). But while on Cu(111) the surface state remains recognizable even with the tip contributions, it is distorted beyond recognition on Ag(111). In the case of a sharp tip, the main peak is at the lower end of the spectrum. In the case of a flat tip, the energy value of the peak is reproduced, but the onset is substantially extended.

C. Tunneling spectra on Au(111)

The tunneling spectrum on Au(111) shows the onset of the surface state around -500 mV, in agreement with experiments. Also the steeper slope toward higher bias voltages as compared to, e.g., Cu(111) is backed by experimental data.²⁵

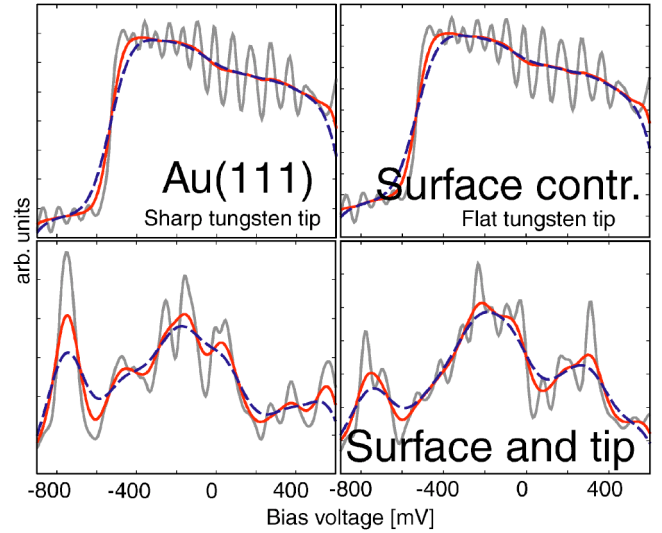


FIG. 5. Differential spectrum on Au(111). The top frames show the surface contribution of the spectrum, simulated with the sharp (left) and flat (right) tip. The bottom frames display the sum of surface and tip contributions. It can be clearly seen that the tip contribution also in this case distorts the spectra and makes the onset of the surface state all but unrecognizable.

In the plots of the surface contributions, the energy resolution of the band map with low thermal broadening (Fig. 5, gray line) can clearly be distinguished. We conclude from the simulations, as in the previous cases, that the band map is precise enough to reproduce experimental spectra in a thermal range above 150 K. Concerning the tip contributions, we note the same problem as on the other surfaces: the peaks introduced by the tip electronic structure, in particular its confinement to a few layers of tungsten, have no correspondence in experimental data.

IV. SURFACE-STATE ONSET AND LIFETIME BROADENING

In the past, two methods to determine the lifetime of surface-state electrons have been suggested. (i) The slope of the surface state onset in a spectrum, which directly relates to the lifetime broadening due to inelastic electron-electron and electron-phonon interactions.³ (ii) The decay of standing waves with the distance from a surface terrace.²⁷ We have calculated the slope of the onset from our spectroscopy simulations and compared the results to experimental low-temperature measurements. In all cases, the spectrum was simulated with an energy resolution of 2 mV, and the ensuing spectrum smoothed with a Gaussian of 10 mV half-width. The results of this comparison are shown in Fig. 6. At first glance, the slope differs for Ag(111) and Cu(111) or Au(111) surface states; the results furthermore seem in acceptable agreement with experimental data.²⁵

However, the theoretical model of our simulations does not include many-body effects. Given that the onset of a surface state should in an ideal case be a step function [see Eq. (12)], there should be no difference between the onset at the three noble metals. But the picture changes if we assume

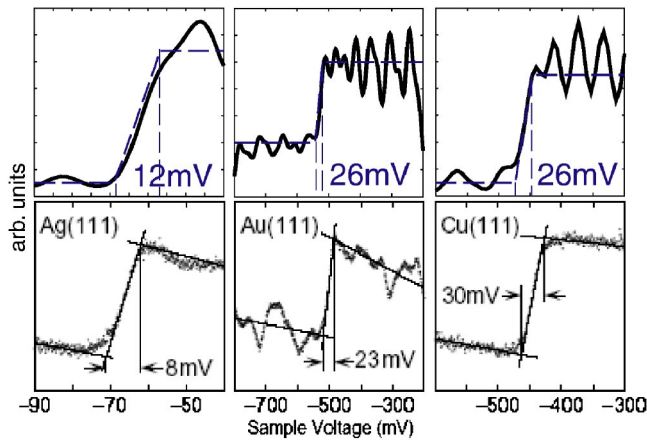


FIG. 6. Onset of surface states on noble metal surfaces. The experimental data (bottom frames) were taken from Ref. 25. The values obtained seem to correspond well with experimental values, even though they relate to the band-structure map rather than inelastic effects, as explained in the text.

that the energy resolution in the spectrum, essentially determined by the band-structure map, is comparable to the onset we determine in the simulation. Then, the dispersion curve of the surface state will provide the energy difference from one k point of the band-structure map to the next. And if the dispersion curve has a very low curvature at the $\bar{\Gamma}$ point, then the energy resolution will be improved. This makes the simulated onset for Ag(111) only about half the value obtained for Au(111) and Cu(111). From the viewpoint of comparisons between experiments and simulations with respect to surface-state lifetimes, it seems that a fully adequate comparison requires an even higher resolution of the band-structure map than used in this work. Including many-body effects in such a simulation seems well beyond computational means today. Considering the problem of simulation, it seems to be safe to conclude that a theoretical treatment of lifetime broadening is best applied to the decay of standing waves, e.g., scattered from a step edge rather than to the slope of the surface-state onset. In the latter case it seems unclear, as long as three-dimensional simulations are not viable, how a particular experimental situation will actually influence the achieved onset and thus make a detailed comparison between experiment and theory problematic.

V. DISCUSSION

Given that tunneling spectra on noble metal surfaces have been measured for more than ten years, it seems quite astonishing that only very few detailed comparisons between experiments and simulations have been accomplished (see, for example, Refs. 3, 16, and 26). One reason, as seems clear from the presented theoretical results, is the enormous numerical effort. Tunneling spectra depend to a much higher degree on the numerical details of the electronic structure calculations than topographies.

Concerning the theoretical scheme developed for differential tunneling spectroscopy, it seems accurate enough to describe the detailed features of a spectrum with a resolution of

20–50 mV. For most spectra, this level of accuracy seems sufficient. However, in very detailed low-temperature experiments, experimental accuracy is above this level. In principle, it is possible to increase the number of k points to about 10 000 in the Brillouin zone, and to map the band structure with sufficient accuracy. This has not been done in the present work, which was aimed at introducing the method and showing its potentials. Given the theoretical results presented in this paper, it seems fair to consider differential spectroscopy, even if it is based on an approximation for the bulk of electron transitions—that they will not be influenced substantially by the change of transition channels due to the offset of bias—as a quite accurate tool in simulating tunneling spectra. The additional advantages, i.e., the detailed analysis of surface and tip contributions, the comparatively high efficiency, and the numerical stability, more than balance the approximation involved.

Concerning the tip electronic structure, the simulations reveal a lack of detailed understanding. It was shown in previous simulations that tunneling topographies can be accurately simulated with STM tip models of a rather limited size. This, however, is not possible in tunneling spectroscopy or only under specific conditions. If, for example, the density of states at the Fermi level of the surface system is very low, the second term in Eq. (6) becomes very small compared to the first term. Since this second term describes the contributions of the tip band structure to the differential spectrum, it will become negligible compared with the overlap of the surface electronic structure and tip states near the Fermi level. In this case, the simulated tunneling spectrum will be essentially the spectrum of the surface alone. This applies in particular to metal surfaces with a surface state far from the Fermi level and semiconductor surfaces. First simulations of these surfaces will be presented in the very near future and it will be shown that in this case it is possible to simulate the full spectrum including the STM tip.

If the problem of suitable tip electronic structures, analyzed with this method, remained unsolved, the method of Lang,¹² using only the surface electronic structure, would be the end point of any analysis. But the advantage of the suggested scheme is that it allows quantifying a large class of materials where the tip electronic structure, even with Bardeen's method, is not too relevant: these are all materials like semiconductors or certain magnets, where the surface density of states at the Fermi level is very low by comparison. It also tells us, via the analysis of surface states and their numerical representation, that the band structure of a surface is only correctly represented if the calculation involves at least 23 layers. And finally it allows a qualification of tip electronic structures, which will faithfully represent even complicated surfaces: this is always the case if the tip electronic structure has a sharp peak at the Fermi level. In this case, the second term in Eq. (6) is equally negligible. That such tip structures may exist can be inferred from the reduction of the valence band if atoms have a decreased number of nearest neighbors, as, e.g., at surfaces. Reducing this number further, e.g., for a tip apex of very few atoms, and increasing the number of layers as well as the size of the tip unit cell, should eventually produce such a structure in simulations. It thus provides a clear research program for how we can in-

clude the tip electronic structure and what these tips, geometrically and electronically, will look like. Improving the electronic structure of the STM tip relies on an accurate map of a semi-infinite tip crystal with a distinct apex structure of a few atoms. Given the numerical limitations, such a tip cannot, at present, be calculated within standard DFT methods, relying, e.g., on a three-dimensional repeat unit. Given the fact that the surface of, e.g., Ag(111) has to be simulated by a film of at least 23 atomic layers, and considering that a single layer of a model tip includes at least eight atoms, an exact map with a high number of k points is unfeasible with current simulation methods. A potential way to improve this situation is to compute the tip electronic structure with non-standard methods, e.g., the Korringa-Kohn-Rostoker method, which can routinely be applied to semi-infinite systems. However, this method is usually limited to only a few atoms per layer and a comparatively low number of k points. Whether or not it can be applied to the specific geometry and composition of the STM tip has to be determined in future calculations.

VI. SUMMARY

In this paper, we have presented a method to calculate the tunneling spectra on metal surfaces. The advantage of the

method is that it includes the full electronic structure of the surface and the STM tip. It allows us, however, to distinguish between surface and tip contributions in the ensuing dI/dV map. The method was applied to differential spectra on (111) noble metal surfaces, where it was shown that we obtain good agreement between theory and simulations. We also showed that the usual STM tip models, successful, e.g., for tunneling topographies, are unsuitable for detailed comparisons between experiment and theory in this case. The reason, identified by a careful analysis of the ensuing spectra, is the local limitation of STM tip structures, leading to confinement of tip electrons and artifacts in the electronic tip structures. A potential improvement of the method is to base the STM tip structure on simulations of semi-infinite systems.

ACKNOWLEDGMENTS

Helpful discussions with A. Arnau, P. Echenique, R. Miranda, and A. L. Vazquez de Parga are gratefully acknowledged. W.A.H. thanks the Royal Society for financial support. A.G.L. is funded by the European Commission.

*Electronic address: whofer@liverpool.ac.uk

¹D. M. Eigler and E. K. Schweizer, *Nature (London)* **344**, 524 (1990).

²K.-F. Braun and K.-H. Rieder, *Phys. Rev. Lett.* **88**, 096801 (2002).

³J. Kliewer, R. Berndt, E. V. Chulkov, V. M. Silkin, P. M. Echenique, and S. Crampin, *Science* **288**, 1399 (2000).

⁴W. A. Hofer, A. S. Foster, and A. L. Shluger, *Rev. Mod. Phys.* **75**, 1287 (2003).

⁵F. Calleja, A. Arnau, J. J. Hinarejos, A. L. Vazquez de Parga, W. A. Hofer, P. M. Echenique, and R. Miranda, *Phys. Rev. Lett.* **92**, 206101 (2004).

⁶V. L. Moruzzi, J. F. Janak, and A. R. Williams, *Calculated Electronic Properties of Metals* (Pergamon Press, New York, 1978).

⁷R. F. Feenstra, *Surf. Sci.* **299/300**, 965 (1994).

⁸W. A. Hofer and J. Redinger, *Surf. Sci.* **447**, 51 (2000).

⁹J. Bardeen, *Phys. Rev. Lett.* **6**, 57 (1961).

¹⁰C. Julian Chen, *Introduction to Scanning Tunneling Microscopy* (Oxford University Press, Oxford, 1993).

¹¹J. Tersoff and D. R. Hamann *Phys. Rev. B* **31**, 805 (1985).

¹²N. D. Lang, *Phys. Rev. B* **34**, 5947 (1986).

¹³J. A. Stroscio, D. T. Pierce, A. Davies, R. J. Celotta, and M. Weinert, *Phys. Rev. Lett.* **75**, 2960 (1995).

¹⁴A. Biedermann, O. Genser, W. Hebenstreit, M. Schmid, J.

Redinger, R. Podloucky, and P. Varga, *Phys. Rev. Lett.* **76**, 4179 (1996).

¹⁵J. Li, and W.-D. Schneider, R. Berndt, and B. Delley, *Phys. Rev. Lett.* **80**, 2893 (1998).

¹⁶G. Hörmandinger, *Phys. Rev. B* **49**, 13 897 (1994).

¹⁷G. Kresse and J. Hafner, *Phys. Rev. B* **47**, 558 (1993).

¹⁸G. Kresse and J. Furthmüller, *Phys. Rev. B* **54**, 11 169 (1996).

¹⁹P. E. Blöchl, *Phys. Rev. B* **50**, 17 953 (1994).

²⁰J. P. Perdew *et al.*, *Phys. Rev. B* **46**, 6671 (1991).

²¹G. Nicolay, F. Reinert, S. Hüfner, and P. Blaha, *Phys. Rev. B* **65**, 033407 (2001).

²²L. M. Molina, M. D. Rasmussen, and B. Hammer, *J. Chem. Phys.* **120**, 7673 (2004).

²³D. C. Meier and D. W. Goodman, *J. Am. Chem. Soc.* **126**, 1892 (2004).

²⁴F. Reinert, *J. Phys.: Condens. Matter* **15**, S693 (2003).

²⁵P. M. Echenique, R. Berndt, E. V. Chulkov, Th. Fauster, A. Goldmann, and U. Höfer, *Surf. Sci. Rep.* **52**, 219 (2004).

²⁶A. L. Vazquez de Parga, O. S. Hernan, R. Miranda, A. Levy Yeyati, N. Mingo, A. Martin-Rodero, and F. Flores, *Phys. Rev. Lett.* **80**, 357 (1998).

²⁷L. Burgi, H. Brune, O. Jeandupeux, and K. Kern, *J. Electron Spectrosc. Relat. Phenom.* **109**, 33 (2000).